Supplemental Methods

Genotyping

Genotyping was performed as described previously (1). The genotyping primers included: Cdh5 Cre, 5' GCCTGCATTACCGGTCGATGCAACGA, 3' GTGGCAGATGGCGCGGCAACACCATT; TRPV4^{loxP}, 5' TGAAATCTGACCTCTTGTCCCC, 3' TTGTGTACTGTCTGCACACCAGGC; Cav-1^{loxP}, F1" 5'-TTCTGTGTGCAAGCCTTTCC-3', R1" 5'-GTGTGCGCGTCATACACTTG-3'; SMC Cre, F 5' TGACCCCATCTCTTCACTCC, R 5' AGTCCCTCACATCCTCAGGTT. All primers were ordered from Eurofins Genomics (Louisville, KY).

Cardiac Magnetic Resonance Imaging (MRI)

MRI studies were conducted under protocols that comply with the Guide for the Care and Use of Laboratory Animals (NIH publication no. 85-23, Revised 1996). Mice were positioned in the scanner under 1.25% isoflurane anesthesia and body temperature was maintained at 37°C using thermostatic circulating water. A cylindrical birdcage RF coil (Bruker, 30 mm-diameter) with an active length of 70 mm was used, and heart rate, respiration, and temperature were monitored during imaging using a fiber optic, MR-compatible system (Small Animal Imaging Inc., Stony Brook, NY). MRI was performed on a 7 Tesla (T) Clinscan system (Bruker, Ettlingen, Germany) equipped with actively shielded gradients with a full strength of 650 mT/m and a slew rate of 6666 mT/m/ms (2). Six short-axis slices were acquired from base to apex, with slice thickness of 1 mm, in-plane spatial resolution of 0.2 × 0.2 mm^2, and temporal resolution of 8–12 ms. Baseline ejection fraction (EF), end-diastolic volume (EDV), end-systolic volume (ESV), myocardial mass, wall thickness, stroke volume, and cardiac output were assessed from the cine images using the freely available software Segment version 2.0 R5292 (http://segment.heiberg.se).

Right ventricular systolic pressure (RVSP) and Fulton Index measurement

Mice were anesthetized with pentobarbital (50 mg/kg bodyweight; intraperitoneally) and bupivacaine HCl (100 μL of 0.25% solution, subcutaneously) was used to numb the dissection site on the mouse. RVSP was measured as an indirect indicator of pulmonary arterial pressure (PAP). A Mikro-Tip pressure catheter (SPR-671; Millar Instruments, Huston, TX), connected to a bridge amp (FE221), and a PowerLab 4/35 4-channel recorder (Instruments, Colorado Springs, CO), was cannulated through the external jugular vein into the right ventricle. Right ventricular pressure was acquired and analyzed using LabChart8 software (ADInstruments, Colorado Springs, CO). A stable 3-minute recording was acquired for all animals, and 1-minute continuous segment was used for data analysis. When necessary, traces were digitally filtered using a low-pass filter at a cut-off frequency of 50 Hz. At the end of the experiments, mice were euthanized, and the hearts were isolated for right ventricular hypertrophy analysis. Right ventricular hypertrophy was determined by calculating the Fulton Index, a ratio of the right ventricular (RV) heart weight over the left ventricular (LV) plus septum (S) weight (RV/ LV+S).

Measurement of Pulmonary arterial pressure (PAP)

PAP was evaluated using an IPL-1 ex vivo murine lung perfusion system (Harvard Apparatus, Holliston, MA) as previously described (3). Briefly, mice were anesthetized using isoflurane. A tracheostomy was performed, and animals were ventilated with room air at 150 strokes/min and a stroke volume of 200 μL. Animals were exsanguinated by transecting the inferior vena cava. The main pulmonary artery was cannulated through the right ventricle, and the left ventricle was tube-vented through a small incision at the apex of the heart. The lungs were then perfused at constant flow of 0.5 cc·min−1 with Krebs-Henseleit buffer containing 0.2% Glucose, 0.014% Magnesium Sulfate, 0.016% Monopotassium Phosphate, 0.035% Potassium Chloride, 0.69% Sodium Chloride, 373 μg/mL Calcium Chloride, and 2.1% Sodium Carbonate. The perfusate

buffer and isolated lungs were maintained at 37°C using a circulating water bath. Once properly perfused and ventilated, the isolated lungs were maintained on the system for a 10-minute equilibration period, after which, hemodynamic and pulmonary parameters were recorded by the PULMODYN data acquisition system (Hugo Sachs Elektronik, Breisgau, Germany).

Quantitative polymerase chain reaction (qPCR)

EC sheets were used for mRNA isolation as described previously (4). Approximately 10 4^{th}-order PAs were enzymatically digested in dissociation solution (in mmol/L, 55 NaCl, 80 Na-glutamate, 6 KCl, 2 $MgCl_2$, 0.1 $CaCl_2$, 10 glucose, 10 HEPES, pH 7.3) containing Worthington neutral protease (0.5 mg/mL) 30 minutes at 37°C. Following enzymatic digestion, EC sheets were gently squeezed out from the arterial wall by using fine tips of 1 mL syringe needles. EC sheets were plated on a patch clamp chamber and allowed to settle down for 10-15 minutes at room temperature. EC sheets were collected with a micropipette (~ 0.5-0.8 MΩ) applying gentle suction. The purity of EC sheets was confirmed with FITC-tagged CD31 staining in control experiments. Isolated ECs (~ 2000) were transferred to RTL buffer with β-mercapto ethanol and snap-frozen in liquid nitrogen. RNA isolation and qPCR were performed as described previously (1). Data were analyzed using the $\Delta\Delta C_t$ method. qPCR primers for Cav-1, TRPV4, iNOS and NOX1 were ordered from Eurofins Genomics (Louisville, KY). For verifying the smooth muscle cell knockout, mRNA was extracted from endothelium-denuded arteries and qPCR performed as described above.

Pressure Myography

Mouse and human PAs (~ 50 μm) were cannulated on glass micropipettes in a pressure myography chamber (The Instrumentation and Model Facility, University of Vermont, Burlington, VT), and were pressurized at a physiological pressure of 15 mm Hg (5). Arteries were superfused with PSS (in mmol/L, 119 NaCl, 4.7 KCl, 1.2 KH_2PO_4, 1.2 $MgCl_2$ hexahydrate, 2.5

$CaCl_2$ dihydrate, 7 dextrose, and 24 $NaHCO_3$) at 37°C and bubbled with 20% O_2/5% CO_2 to maintain the pH at 7.4. PAs were pre-constricted with 50 nmol/L U46619 (a thromboxane A2 receptor agonist). Before measurement of vascular reactivity, arteries were treated with NS309 (1 μmol/L), a direct opener of endothelial IK/SK channel, to assess endothelial health. Arteries that failed to dilate to NS309 were discarded. Changes in arterial diameter were recorded at a 60-ms frame rate using a charge-coupled device camera and edge-detection software (IonOptix LLC, Westwood, MA) (6, 7). At the end of each experiment, Ca^{2+}-free PSS (in mmol/L, 119 NaCl, 4.7 KCl, 1.2 KH_2PO_4, 1.2 $MgCl_2$ hexahydrate, 7 dextrose, 24 $NaHCO_3$, and 5 EGTA) was applied to assess the maximum passive diameter. Percent constriction was calculated by:

$$[(Diameter_{before} - Diameter_{after})/Diameter_{before}] \times 100,$$

where $Diameter_{before}$ is the diameter of the artery before a treatment and $Diameter_{after}$ is the diameter after the treatment. Percent dilation was calculated by:

$$[(Diameter_{dilated} - Diameter_{basal})/(Diameter_{Ca-free} - Diameter_{basal})] \times 100,$$

where $Diameter_{basal}$ is the stable diameter before drug treatment, $Diameter_{dilated}$ is the diameter after drug treatment, and $Diameter_{Ca\text{-}free}$ is the maximum passive diameter.

Ca^{2+} Imaging

Measurements of $TRPV4_{EC}$ Ca^{2+} sparklets in the intact endothelium of mouse and human PAs were performed as previously described (6). Briefly, PAs (~ 50 μm) were pinned down *en face* on a Sylgard block and loaded with fluo-4-AM (10 μmol/L) in the presence of pluronic acid (0.04%) at 30°C for 30 minutes. $TRPV4_{EC}$ Ca^{2+} sparklets were recorded at 30 frames per second with

Andor Revolution WD (with Borealis) spinning-disk confocal imaging system (Oxford Instruments, Abingdon, UK) comprised of an upright Nikon microscope with a 60X water dipping objective (numerical aperture 1.0) and an electron multiplying charge coupled device camera (iXon 888, Oxford Instruments, Abingdon, UK). All experiments were carried out in the presence of cyclopiazonic acid (20 μmol/L, a sarco-endoplasmic reticulum (ER) Ca^{2+}-ATPase inhibitor) in order to eliminate the interference from Ca^{2+} release from intracellular stores. Fluo-4 was excited at 488 nm with a solid-state laser and emitted fluorescence was captured using a 525/36-nm band-pass filter. $TRPV4_{EC}$ Ca^{2+} sparklets were recorded before and 5 minutes after the addition of specific compounds. The effect of TRPV4 channel inhibitor GSK2193874 (GSK219; 100 nmol/L) on TRPV4 sparklets was confirmed 10 minutes after addition (4, 5). To generate fractional fluorescence (F/F_0) traces, a region of interest defined by a 1.7-μm^2 (5×5 pixels) box was placed at a point corresponding to peak sparklet amplitude. Each field of view was ~ 110×110 μm and covered ~ 15 ECs. Representative F/F_0 traces were filtered using a Gaussian filter and a cutoff corner frequency of 4 Hz. Sparklet activity was assessed as described previously using the custom-designed SparkAn software (6, 7). The traces shown indicate sparklet sites in a representative endothelial cell from each group.

Calculation of TRPV4 Sparklet Activity per Site

Activity of TRPV4 Ca^{2+} sparklets was evaluated as described previously (6, 7). The average number of active TRPV4 channels, as defined by NP_O (where N is the number of channels at a site and P_O is the open state probability of the channel), was calculated by

$$NP_O = (T_{level1} + 2T_{level2} + 3T_{level3} + 4T_{level4}) / T_{total} ,$$

where T is the dwell time at each quantal level detected at TRPV4 sparklet sites and T_{total} is the duration of the recording. NP_O was determined using Single Channel Search module of Clampfit and quantal amplitudes derived from all-points histograms (8) ($\Delta F/F_0$ of 0.29 for Fluo-4–loaded PAs).

To obtain the number of sparklet sites per cell, the total number of sparklet sites in the field of view was divided by the number of endothelial cells in that field of view.

Patch clamp in freshly isolated pulmonary ECs and in HEK293 cells

Fresh ECs were obtained via enzymatic digestion of 4th-order PAs. Briefly, PAs were incubated in the dissociation solution (in mmol/L, 55 NaCl, 80 Na glutamate, 6 KCl, 2 $MgCl_2$, 0.1 $CaCl_2$, 10 glucose, 10 HEPES, pH 7.3) containing Worthington neutral protease (0.5 mg/mL) for 30 minutes at 37°C. The extracellular solution consisted of (in mmol/L) 10 HEPES, 134 NaCl, 6 KCl, 2 $CaCl_2$, 10 glucose, and 1 $MgCl_2$ (adjusted to pH 7.4 with NaOH). The intracellular pipette solution for perforated-patch configuration consisted of (in mmol/L) 10 HEPES, 30 KCl, 10 NaCl, 110 K-aspartate, and 1 $MgCl_2$ (adjusted to pH 7.2 with NaOH). Cells were kept at room temperature in a bathing solution consisting of (in mmol/L) 10 HEPES, 134 NaCl, 6 KCl, 2 $CaCl_2$, 10 glucose, and 1 $MgCl_2$ (adjusted to pH 7.4 with NaOH). Narishige PC-100 puller (Narishige International USA, INC., Amityville, NY, USA) was utilized to pull patch electrodes, which were polished using MicroForge MF-830 polisher (Narishige International USA, INC., Amityville, NY, USA). The pipette resistance was (3–5 ΩM). Amphotericin B was dissolved in the intracellular pipette solution to reach a final concentration of 0.3 μmol/L. The data were acquired using HEKA EPC 10 amplifier and PatchMaster v2X90 program (Harvard Bioscience, Holliston, MA, USA), and analyzed using FitMaster v2X73.2 (Harvard Bioscience, Holliston, MA, USA) and MATLAB R2018a (MathWorks, Natick, MA, USA). TRPV4 channel current was recorded from freshly isolated ECs as described previously (4, 6). Briefly, GSK101-induced outward currents through TRPV4 channels were

assessed in response to a 200-ms voltage step from -45 mV to +100 mV in the presence of ruthenium red in order to prevent Ca^{2+} and activation of IK/SK channels at negative voltages. TRPV4 channel current was recorded in HEK293 cells using whole-cell patch configuration 48 hours after transfection. The intracellular solution consisted (in mmol/L) 20 CsCl, 100 Cs-aspartate, 1 $MgCl_2$, 4 ATP, 0.08 $CaCl_2$, 10 BAPTA, 10 HEPES, pH 7.2 (adjusted with CsOH). Currents were measured using a voltage clamp protocol where voltage-ramp pulses (-100 mV to +100 mV) were applied over 200 ms with a holding potential of -50 mV. TRPV4 currents were measured before or five minutes after treatment with peroxynitrite (5 μmol/L).

Immunostaining

En face PAs (~ 50 μm) were fixed with 4% paraformaldehyde (PFA) at room temperature for 15 minutes and then washed 3 times with phosphate-buffered saline (PBS). The tissue was permeabilized with 0.2% Triton-X for 30 minutes, blocked with 5% normal donkey serum (ab7475, Abcam, Cambridge, MA) or normal goat serum (ab7475, Abcam, Cambridge, MA) for 1 hour at room temperature. PAs were incubated with the primary antibodies (Table 1) overnight at 4°C. Following the overnight incubation, PAs were incubated with secondary antibody 1:500 Alexa Fluor® 568-conjugated donkey anti-rabbit (Life Technologies, Carlsbad, CA, USA) for 1 hour at room temperature in the dark room. For nuclear staining, PAs were washed with PBS and then incubated with 0.3 μmol/L DAPI (Invitrogen, Carlsbad, CA, USA) for 10 minutes at room temperature. Images were acquired along the z-axis from the surface of the endothelium to the bottom where the EC layer encounters the smooth muscle cell layer with a slice size of 0.1 μm using the Andor microscope described above. ECs were co-stained with fluorescent anti-CD31 antibody, and SMCs were co-stained with anti-α-actin antibody (Table below). The co-staining was evaluated using an excitation of 488 nm and collecting the emitted fluorescence with a 525/36 nm band-pass filter. Immunostaining was evaluated using an excitation of 561 nm and collecting

the emitted fluorescence with a 607/36 nm band-pass filter. DAPI immunostaining was evaluated using an excitation of 409 nm and collecting the emitted fluorescence with a 447/69 nm band-pass filter. Negative control experiments were performed using arteries from endothelium-specific (TRPV4, Cav-1) and global knockout (NOX1, iNOS) mice.

List of antibodies used in this study.

Protein	Product no.	Company	Clonality	Concentration
CD-31	RM5201	Invitrogen, Carlsbad, Ca, USA	Monoclonal	1:100
α-actin	F3777	Sigma Aldrich, St. Louis, MO, USA	Monoclonal	1:500
TRPV4	LSC 94498	LifeSpan BioScience INC	Polyclonal	1:200
Cav-1	Ab2910	Abcam plc.	Polyclonal	1:500
Cav-1 (PLA only)	NB100-615	Novus Biologicals, LLC	Monoclonal	1:200
iNOS	NB300-605	Novus Biologicals, LLC	Polyclonal	1:500
NOX1	NBP1-31546	Novus Biologicals, LLC	Polyclonal	1:500

In situ Proximity Ligation Assay (PLA)

En face PAs (~ 50 μm) were fixed with 4% PFA for 15 minutes followed by 3 washes with PBS. PAs were then permeabilized with 0.2% Triton X for 30 minutes at room temperature followed by blocking with 5% normal donkey serum (Abcam plc, Cambridge, MA, USA) and 300 mmol/L glycine for 1 hour at room temperature. After 3 washes with PBS, PAs were incubated with the primary antibodies (SI appendix Table 1) overnight at 4 °C. The PLA protocol from Duolink PLA

Technology kit (Sigma-Aldrich, St. Louis, MO, USA) was followed for the detection of co-localized proteins. Lastly, PAs were incubated with 0.3 μmol/L DAPI nuclear staining (Invitrogen, Carlsbad, CA, USA) for 10 minutes at room temperature in the dark room. PLA images were acquired using the Andor Revolution spinning-disk confocal imaging system along the z-axis at a slice size of 0.1 μm. Images analysis was performed using IMARIS version 9.3. Images were analyzed by normalizing the number of positive puncta by the number of nuclei in a field of view. Negative control experiments were performed using arteries from endothelium-specific (TRPV4, Cav-1) and global knockout (NOX1, iNOS) mice (1).

DAF-FM, nitric oxide (NO) measurements

DAF-FM (4-amino-5 methylamino-2',7'-difluorofluorescein diacetate) was dissolved in HEPES-PSS containing 0.02% pluronic acid (8) to obtain a solution with final concentration of 5 μmol/L. Fourth-order PAs were pinned down *en face* on a Sylgard block, and loaded with 5 μmol/L DAF-FM for 20 minutes at 30°C in the dark. DAF-FM, following NO binding, forms a fluorescent traizole compound. DAF-FM was excited at 488 nm, and emission was collected with a 525/36-nm band-pass filter. Images were captured across the z-axis with a slice thickness of 0.1 μm from the surface of the endothelium to the bottom where the endothelium cell layer encounters the smooth muscle cell layer. GSK101-induced NO release was studied as follows: PAs were incubated at 30°C with GSK101 (or vehicle only) for 5 minutes, successively PAs were treated with GSK101 + DAF-FM (or vehicle + DAF-FM) for 20 minutes. SparkAn software was used to analyze DAF-FM images. An outline was manually drawn around each endothelial cell to measure the arbitrary fluorescent intensity per cell. Background fluorescence (intensity without laser) was subtracted from the arbitrary fluorescent value obtained for each cell. Fluorescence values of each cell were averaged to obtain a single fluorescence number for the specific field.

Plasmid generation and transfection into HEK293 cells

Generation of TRPV4 plasmids has been described previously (1). Wild-type Cav-1 and Cav-1 mutants Cav-1^{C133A}, Cav-1^{C143A}, Cav-1^{C156A} were obtained from Origene Technologies (Montgomery County, MD).

Peroxynitrite imaging

Peroxynitrite was prepared and used in vascular experiments as described previously (4, 9). Coumarin boronic acid (CBA), a peroxynitrite-specific fluorescent indicator was used for non-confocal peroxynitrite imaging (4). Peroxynitrite oxidizes CBA into the fluorescent product 7-hydroxycoumarin (COH). CBA reacts with peroxynitrite at exponentially faster rates than hydrogen peroxide and hypochlorous acid. Fourth-order PAs were pinned down *en face*, and were incubated with CBA (20 μmol/L) for 30 minutes at room temperature. Non-confocal images were obtained by exciting endothelial COH was at 340 nm (CoolLED, pE-340^{fura}, Andover, UK). Emitted fluorescence was captured at room temperature using a 447/60 nm band-pass filter, Nikon fluor 40X objective, and Andor electron multiplying charge coupled device camera. The fluorescent intensity was averaged for the whole field of view and compared between experimental groups. Each data point represents one field of view. At least 3 arteries were used for each treatment.

Co-Immunoprecipitation

HEK 293T cells were co-transfected either with mouse NOX1 (Myc-DDK-tagged; Cat# MR226022, Origene) or NOS2 (Myc-DDK-tagged; Cat# MR211704, Origene) along with Cav1(Flag-tagged; Cat# MG53027-CF, Sino Biological) expression vectors for 48 hours. Cells were lysed using immunoprecipitation compatible lysis buffer (IP-lysis buffer contains in mmol/L, 50 HEPES, 200 KCl, 2 EDTA, 1 MgCl2, 0.5 % Triton X-100, 10 % glycerol, and protease inhibitors cocktail). Cellular lysates from the 293T cells that were not transfected with Cav1 or NOX1or

NOS2 were used as a negative control. Cell lysates were separated from insoluble cell debris by centrifugation at 12000g for 10 minutes. The pierce anti-c-Myc magnetic beads (Cat# 88842) were used to pull down Myc-tagged NOX1 or NOS2. Briefly, 100 μL of anti-c-Myc magnetic beads were transferred into 1.5 mL tubes. The beads were washed thrice by adding 300 μL of IP-lysis buffer (without protease inhibitors). Cell lysates (1.3 mL) were added to the pre-washed magnetic beads and incubated for 1 hour on the rotating shaker at room temperature. The bound portion to the magnetic beads was collected by placing the tubes on the magnetic stand. The beads were washed three times by adding 500 μL of IP-lysis buffer (without protease inhibitors). The bound portion was eluted by incubating beads in 50 μL of SDS-PAGE sample buffer at 900C for 10 minutes. The elutes were separated and subjected to Western blot analysis using anti-FLAG-HRP (A8592, Sigma Aldrich), anti-c-Myc (NBP1-31546, ThermoFisher) and anti-NOX1 (NBP1-31546, Novus) antibodies.

Drugs and Reagents

Cyclopiazonic acid (CPA), GSK2193874, GSK1016790A and NS309 were purchased from Tocris Bioscience (Minneapolis, MN). Diaminofluorescein-FM diacetate (DAF-FM) and Fluo-4-AM (Ca^{2+} indicator) were purchased from Invitrogen (Carlsbad, CA). NOXA1ds and hypochlorous acid were purchased from Merck KGaA (Darmstadt, Germany). Tempol was purchased from Enzo Life Sciences, Inc. (Farmingdale, NY). Peroxynitrite, uric acid (UA), Fe (III)5,10,15,20-tetrakis (4-sulfonatophenyl)-porphyrinato chloride (FeTPPS), 1400W, spermine NONOate, ebselen, mitoQ, Gö-6976 and U46619 were purchased from Cayman Chemicals (Ann Arbor, MI, USA). gp91 ds-tat was purchased from AnaSpec (Fremont, CA, USA). Catalase-polyethylene glycol (PEG catalase), tamoxifen, sugen (SU5416) xanthine oxidase, hypoxanthine, and taurine were obtained from Sigma-Aldrich (St. Louis, MO).

Statistics

Results are presented as mean ± SEM. N=1 was defined as one artery in the imaging experiments (Ca^{2+} imaging, immunofluorescence, peroxynitrite/NO measurements, PLA), one cell for patch clamp experiments, one mouse for PAP measurements, one artery for pressure myography experiments, and one mouse for qPCR experiments. The data were obtained from at least three mice in experiments performed in at least two independent batches. All data are shown in graphical form using CorelDraw Graphics Suite X7 (Ottawa, ON, Canada) and statistically analyzed using GraphPad Prism 8.3.0 (Sand Diego, CA). A power analysis to determine group sizes and study power (>0.8) was performed using GLIMMPSE software (α=0.05; >20% change). Using this method, some experiments required n=3, while others required n≥4. A Shapiro-Wilk test was performed to determine normality. The data in this article were normally distributed; therefore, parametric statistics were performed. Data were analyzed using two-tailed, paired or independent t-test (for comparison of data collected from two different treatments), one-way ANOVA or two-way ANOVA (to investigate statistical differences among more than two different treatments). Tukey correction was performed for multiple comparisons with one-way ANOVA, and Bonferroni correction was performed for multiple comparisons with two-way ANOVA. Statistical significance was determined as a P value less than 0.05.

Supplemental Table 1.

N = 5 mice	$TRPV4^{fl/fl}$	$TRPV4_{EC}^{-/-}$
End diastolic wall thickness (mm)	0.90 ± 0.04	0.83 ± 0.02
End systolic wall thickness (mm)	1.11 ± 0.04	1.10 ± 0.07
End diastolic volume (μl)	51.43 ± 5.59	57.40 ± 6.50
End systolic volume (μl)	21.54 ± 3.53	25.07 ± 4.94
Left ventricular mass (mg)	80.18 ± 3.05	82.81 ± 6.48
R-R interval (ms)	124.34 ± 6.00	125.63 ± 6.69
Heart Rate	490.19 ± 11.20	479.35 ± 8.69

Supplemental Table 1. Functional MRI analysis of cardiac function in $TRPV4^{fl/fl}$ and $TRPV4_{EC}^{-/-}$ mice. Averaged end diastolic and systolic wall thickness (mm), end diastolic and systolic volume (μL), left ventricular mass, R-R interval (ms), and heart rate. Data represented as mean ±SEM, n = 5.

Supplemental Table 2.

Group	$TRPV4_{EC}$ sparklet sites per cell
N, baseline	0.20 ± 0.03 (5)
N, 10 nM GSK101	2.20 ± 0.16 (5)
N, 30 nM GSK101	3.00 ± 0.14 (5)
CH, baseline	0.07 ± 0.02 (5)* vs N
CH, 10 nM GSK101	0.66 ± 0.12 (5)*** vs N
CH, 30 nM GSK101	3.09 ± 0.15 (5)
Su + CH, baseline	0.08 ± 0.02 (5)* vs N
Su + CH, 10 nM GSK101	0.67 ± 0.07 (5)*** vs N
Su + CH, 30 nM GSK101	3.18 ± 0.24 (5)
Non-PAH, 10 nM GSK101	0.45 ± 0.06 (4)
Non-PAH, 30 nM GSK101	0.94 ± 0.12 (4)
PAH, 10 nM GSK101	0.11 ± 0.04 (4)** vs Non-PAH
PAH, 30 nM GSK101	0.38 ± 0.07 (4)** vs Non-PAH

Supplemental Table 2. Mean values for $TRPV4_{EC}$ sparklet sites per endothelial cell. $TRPV4_{EC}$ sparklet sites per cell in *en face* preparations of PAs from mice exposed to normoxia (N), chronic hypoxia (CH; 3 weeks; 10% O_2) and CH + SU5416 (Su+CH), and Non-PAH and PAH patients (n = 4-5; * P <0.05, ** P <0.01, and *** P <0.001 significance indicated in the table; one-way ANOVA).

Supplemental Table 3.

Group	$TRPV4_{EC}$ sparklet sites per cell
CH, 1 nM GSK101	
- NOXA1ds	0.14 ± 0.04 (5)
+ NOXA1ds	0.59 ± 0.04 (5)*** vs –NOXA1ds
Su + CH, 1 nM GSK101	
- NOXA1ds	0.13 ± 0.02 (5)
+ NOXA1ds	0.53 ± 0.03 (5)*** vs –NOXA1ds
CH, 1 nM GSK101	
- gp91 ds-tat	0.19 ± 0.05 (5)
+ gp91 ds-tat	0.24 ± 0.02 (5)
Su + CH, 1 nM GSK101	
- gp91 ds-tat	0.17 ± 0.03 (5)
+ gp91 ds-tat	0.21 ± 0.02 (5)
CH, 1 nM GSK101	
- MitoQ	0.20 ± 0.06 (5)
+ MitoQ	0.25 ± 0.02 (5)
Su + CH, 1 nM GSK101	
- MitoQ	0.14 ± 0.03 (5)
+ MitoQ	0.20 ± 0.03 (5)
WT Su + CH, 1 nM GSK101	0.13 ± 0.02 (5)
$NOX1^{-/-}$ Su + CH, 1 nM GSK101	0.49 ± 0.04 (5)*** vs WT
$NOX1^{-/-}$, normoxic, 1 nM GSK101	0.43 ± 0.03 (4)
PAH, 10 nM GSK101	
- NOXA1ds	0.10 ± 0.04 (4)
+ NOXA1ds	0.46 ± 0.07 (4)*** vs – NOXA1ds
Su + CH, 1 nM GSK101	

- 1400W	0.16 ± 0.05 (5)
+ 1400W	0.52 ± 0.03 (5)*** vs -1400W
PAH, 10 nM GSK101	
- 1400W	0.16 ± 0.02 (4)
+ 1400W	0.48 ± 0.04 (4)*** vs -1400W
WT Su + CH, 1 nM GSK101	0.15 ± 0.05 (5)
iNOS$^{-/-}$ Su + CH, 1 nM GSK101	0.52 ± 0.08 (5)*** vs WT
CH, 1 nM GSK101	
- UA	0.16 ± 0.03 (5)
+ UA	0.51 ± 0.05 (5)*** vs – UA
Su + CH, 1 nM GSK101	
- UA	0.20 ± 0.06 (5)
+ UA	0.55 ± 0.06 (5)** vs - UA
Cav-1$_{EC}^{-/-}$, Su + CH	
- UA	0.20 ± 0.06 (5)
+ UA	0.22 ± 0.05 (5)
Cav-1$^{fl/fl}$, 10 nM GSK101	
- PN	2.12 ± 0.12 (5)
+ PN	0.57 ± 0.06 (5)*** vs -PN
Cav-1$_{EC}^{-/-}$, 10 nM GSK101	
- PN	0.59 ± 0.16 (5)
+ PN	0.56 ± 0.15 (5)

Supplemental Table 3. Mean values for TRPV4$_{EC}$ sparklet sites per endothelial cells. TRPV4$_{EC}$ sparklet sites per cell in *en face* preparations of PAs from wild-type (WT), NOX1$^{-/-}$, iNOS$^{-/-}$, Cav-1$^{fl/fl}$ or Cav-1$_{EC}^{-/-}$ mice exposed to normoxia (N), chronic hypoxia (CH; 3 weeks; 10% O_2) or CH + SU5416 (Su+CH) in the absence or presence of NOXA1ds (NOX 1 inhibitor; 1 μmol/L), gp91 ds-tat (NOX2 inhibitor; 1 μmol/L), MitoQ (mitochondrial antioxidant; 1 μmol/L), 1400W (iNOS

inhibitor; 1 μmol/L), uric acid (UA; PN scavenger; 200 μmol/L) or peroxynitrite (PN; 5 μmol/L; n = 4-5; *** *P* <0.001 significance indicated in the table; t-test or one-way ANOVA).

Supplemental Figure 1

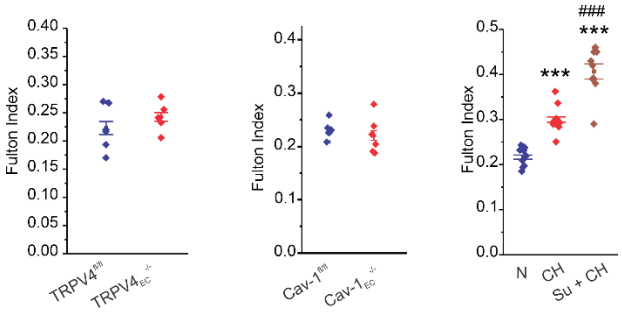

Supplemental Figure 1. Fulton index in $TRPV4_{EC}^{-/-}$, $Cav\text{-}1_{EC}^{-/-}$ and mice exposed to normoxia (N), chronic hypoxia (CH; 3 weeks; 10% O_2), and SU5416 + CH (Su+CH) mice (n = 5-9; *** P <0.001 vs. N; ### P < 0.001 vs. CH; one-way ANOVA).

Supplemental Figure 2

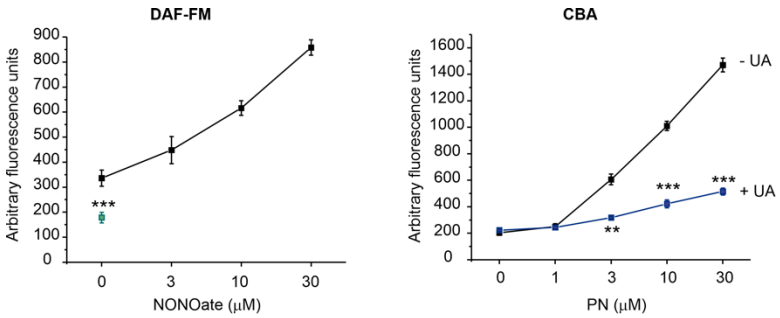

Supplemental Figure 2. Negative and positive controls for DAF-FM and CBA studies. A positive control curve was constructed for DAF-FM using spermine NONOAte (0-30 μmol/L; **left**) and for CBA using peroxynitrite (PN; 0-30 μmol/L; right) in *en face* PAs from C57BL6/J mice. Baseline DAF-FM fluorescence in PAs from eNOS$^{-/-}$ mice (green) was used as a negative control for DAF-FM (n = 5; *** *P* <0.001 vs. C57Bl6/J [0 μmol/L]; two-way ANOVA). CBA imaging in the presence of uric acid (UA, 200 μmol/L) and PN was used as a negative control for CBA (n = 5; ** *P* <0.01 vs. [- UA; 3 μmol/L], *** *P* <0.001 vs. [- UA; 10 and 30 μmol/L]; two-way ANOVA).

Supplemental Figure 3

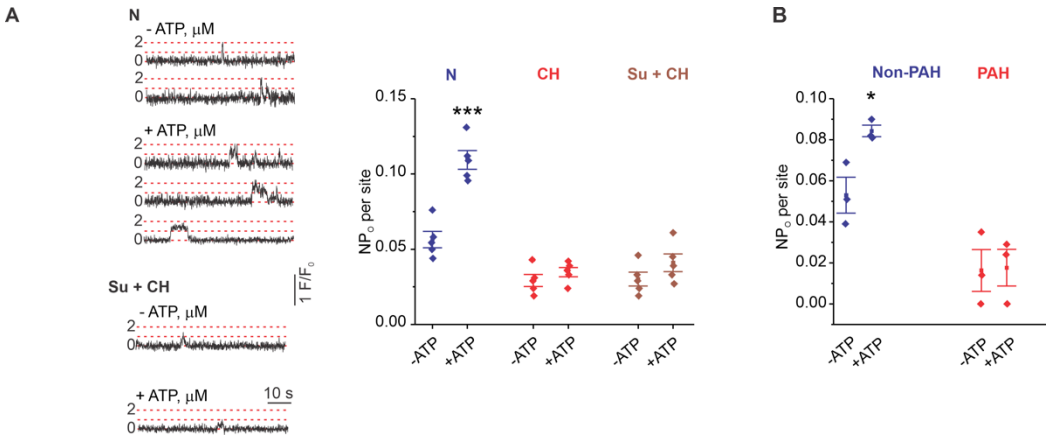

Supplemental Figure 3. A. Left, representative $TRPV4_{EC}$ sparklet traces in *en face* preparations of PAs from mice exposed to normoxia (N) or chronic hypoxia (CH; 3 weeks; 10% O_2) + SU5416 (Su+CH) in the absence or presence of ATP (10 μmol/L). **Right,** $TRPV4_{EC}$ sparklet activity (NP_O) per site in *en face* preparations of PAs from mice exposed to N, CH or Su+CH in the absence or presence of ATP (10 μmol/L), expressed as NP_O per site (n = 5; *** P <0.001 vs. N [- ATP]; two-way ANOVA). N is the number of channels per site and P_O is the open state probability of the channel. Experiments were performed in the presence of cyclopiazonic acid (CPA; 20 μmol/L) to eliminate Ca^{2+} release from intracellular stores. **B.** Effect of ATP (10 μmol/L) on $TRPV4_{EC}$ sparklet traces in *en face* preparations of PAs from Non-PAH and PAH patients, expressed as NP_O per site (n = 3-4; * P < 0.05 vs. Non-PAH [- ATP]; two-way ANOVA).

Supplemental Figure 4

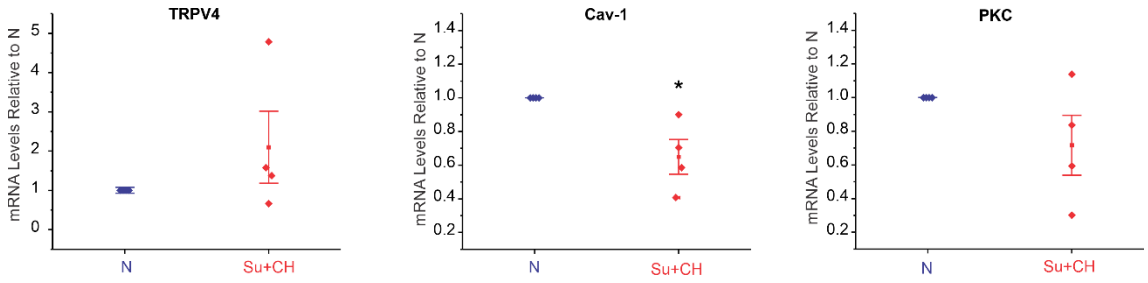

Supplemental Figure 4. Expression of TRPV4, Cav-1, and PKC in endothelial cells (EC) from normal and PH mice. Endothelial mRNA levels of TRPV4 (**left**) and Cav-1 (**center**) and PKC (**right**) in mice exposed to normoxia (N) and chronic hypoxia (CH; 3 weeks; 10% O_2) + SU5416 (Su+CH;), expressed relative to that in N mice (n = 5; * $P < 0.05$ vs. N [Cav-1]; t-test).

Supplemental Figure 5

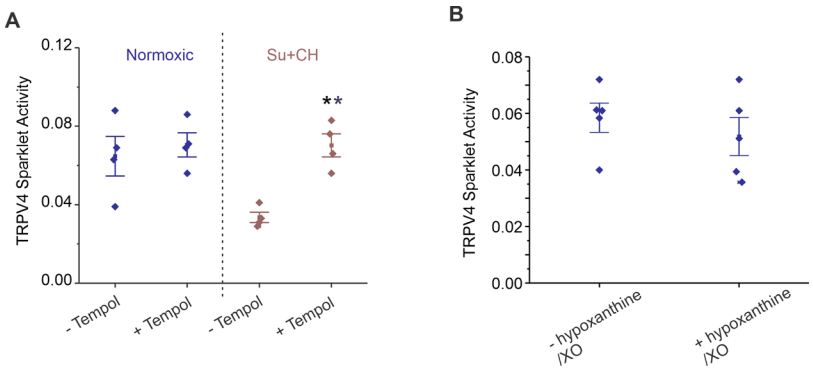

Supplemental Figure 5. Superoxide radicals do not directly inhibit $TRPV4_{EC}$ channel activity in pulmonary arteries. A. $TRPV4_{EC}$ sparklet activity per site (NP_O) in *en face* preparations of PAs from C57BL6/J mice exposed to normoxia (N) and chronic hypoxia (CH; 3 weeks; 10% O_2) + SU5416 (Su+CH) relative to N mice in the absence or presence of $O_2^{\cdot-}$-lowering compound tempol (200 μmol/L). N is the number of channels per site and P_O is the open state probability of the channel. Experiments were performed in the presence of cyclopiazonic acid (CPA, 20 μmol/L) to eliminate Ca^{2+} release from intracellular stores (n = 5; ** $P < 0.01$ vs. Su+CH [– Tempol]; one-way ANOVA). **B.** $TRPV4_{EC}$ sparklet activity per site (NP_O) in *en face* preparations of PAs from N mice in the absence or presence of hypoxanthine (100 μmol/L) / xanthine oxidane (XO; 0.5 U/ml; n = 5).

Supplemental Figure 6

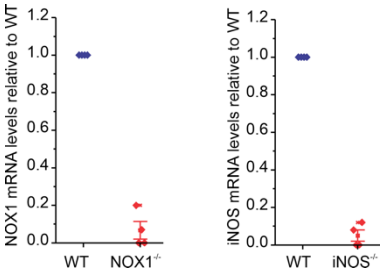

Supplemental Figure 6. Left, Expression of NOX1 at the mRNA level in brain samples from wild-type (WT) and NOX1$^{-/-}$ mice (n=4; *** *P* <0.001 vs. WT; t-test). **Right**, expression of iNOS at the mRNA level in brain samples from WT and iNOS$^{-/-}$ mice (n = 4; *** *P* <0.001 vs. WT; t-test).

Supplemental Figure 7

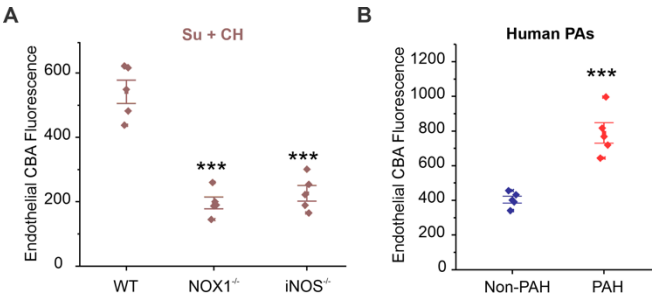

Supplemental Figure 7. NOX1 and iNOS contribute to elevated endothelial levels of PN in mouse model of PH and clinical PAH. Experiments were performed in the presence of PEG-catalase (H_2O_2 metabolizing enzyme; 500 U/ml) and taurine (hypochlorous acid-lowering agent; 1 mmol/L). **A.** endothelial CBA fluorescence in *en face* preparations of 4th-order PAs from WT, NOX1$^{-/-}$ and iNOS$^{-/-}$ mice exposed to chronic hypoxia + SU5416 (Su+CH; n = 5; *** $P < 0.001$ for NOX1$^{-/-}$ vs. WT; *** $P < 0.001$ for iNOS$^{-/-}$ vs. WT; one-way ANOVA). **B**, endothelial CBA fluorescence in *en face* preparations of small PAs from non-PAH and PAH individuals (n = 5; *** $P < 0.001$ vs. non-PAH, t-test).

Supplemental Figure 8

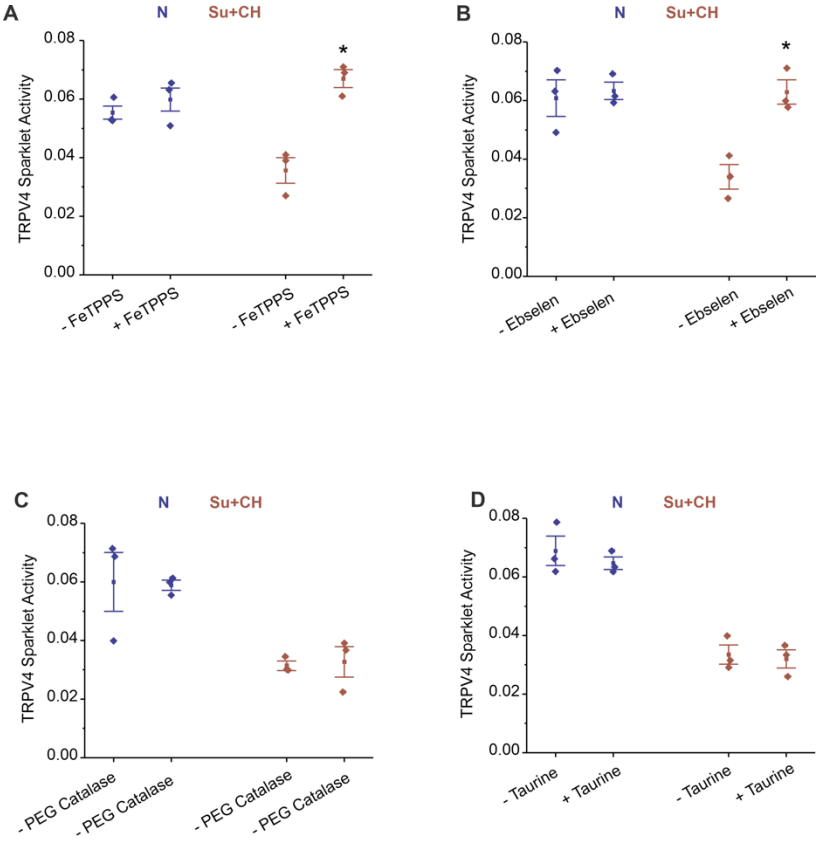

Supplemental Figure 8. Peroxynitrite, but not hydrogen peroxide or hypochlorous acid, reduce $TRPV4_{EC}$ sparklet activity in PAs of PH mice. $TRPV4_{EC}$ sparklet activity GSK101 (3 nmol/L) in *en face* preparations of PAs from mice exposed to normoxic (N) conditions or chronic hypoxia + SU5416 (Su+CH; 3 weeks; 10% O_2), in the absence or presence of FeTPPS (**A**, PN decomposer; 1 μmol/L), Ebselen (**B**, PN scavenger; 1 μmol/L), PEG-catalase (**C**, H_2O_2 metabolizing enzyme; 500 U/ml), or taurine (**D**, hypochlorous acid-lowering agent; 1 mmol/L). Experiments were performed in the presence of cyclopiazonic acid (CPA; 20 μmol/L) to eliminate Ca^{2+} release from intracellular stores (n = 5; * $P < 0.05$ [Su+CH + FeTPPS] vs. – FeTPPS; * $P < 0.05$ [Su+CH + Ebselen] vs. – Ebselen; one-way ANOVA).

Supplemental Figure 9

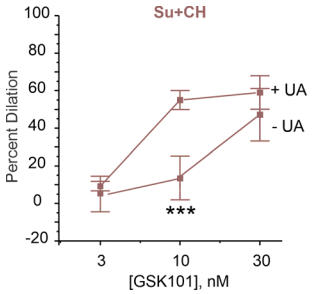

Supplemental Figure 9. Uric acid rescues TRPV4$_{EC}$ channel-induced vasodilation in PH. Effect of uric acid (UA, 200 μmol/L) on GSK101 (3–30 nmol/L)-induced dilation of PAs from C57BL6/J mice exposed to (n = 5; ***P < 0.001 vs. +UA; two-way ANOVA).

Supplemental Figure 10

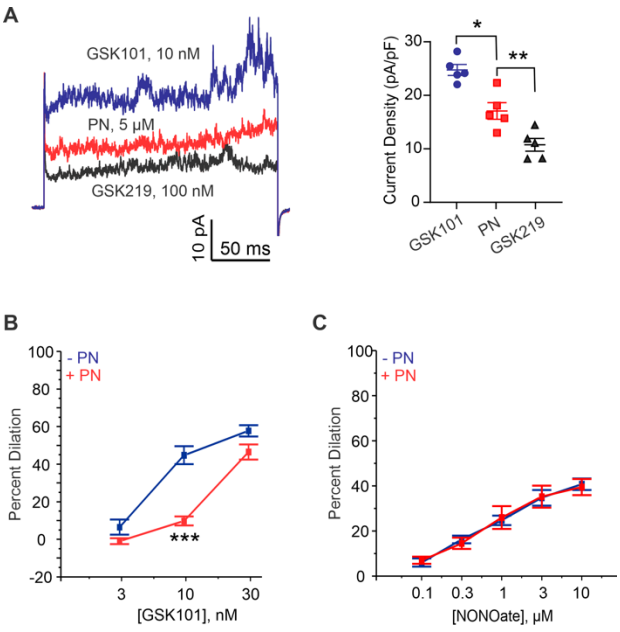

Supplemental Figure 10. PN inhibits $TRPV4_{EC}$ currents and vasodilation, but not NO donor-induced vasodilation. A, **left**, representative GSK1016790A (GSK101; 10 nmol/L)- induced outward $TRPV4_{EC}$ channel currents in freshly isolated ECs from PAs of normal mice. Application of PN (5 μmol/L) or the TRPV4 channel inhibitor GSK219 (100 nmol/L) attenuated $TRPV4_{EC}$ channel currents. $TRPV4_{EC}$ channel currents were evoked by a 200-ms pulse from -50 mV to +100 mV. **Right**, scatter plot showing GSK101-induced outward currents at +100 mV, and inhibition by PN or GSK219 (n = 5; * $P < 0.05$; ** $P < 0.01$; one-way ANOVA). **B**, GSK101 (3–10 nmol/L)-induced dilation of PAs in the absence or presence of PN (5 μmol/L; n = 4; *** $P < 0.001$ vs. -PN; two-way ANOVA). **C**, percent dilation of PAs induced by the NO donor spermine NONOate (0.1–10 μmol/L) in the absence or presence of PN (5 μmol/L; n = 4).

Supplemental Figure 11

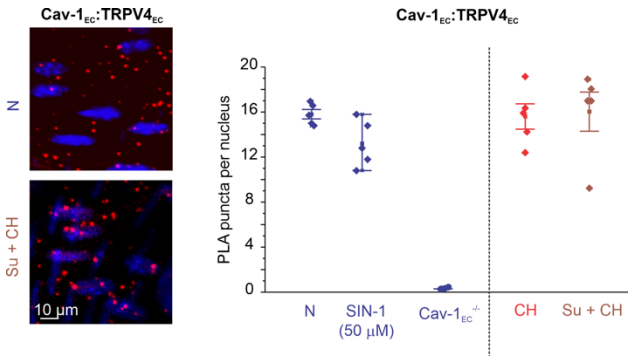

Supplemental Figure 11. Cav-1_{EC}:$TRPV4_{EC}$ localization is not altered in PH. Left, representative *in situ* proximity ligation assay (PLA) results showing merged images of EC nuclei and Cav-1_{EC}:$TRPV4_{EC}$ colocalization (red puncta) in 4th-order PAs from mice exposed to normoxia (N; **top**) and chronic hypoxia (CH; 3 weeks; 10% O_2) + SU5416 (Su+CH; **bottom**) mice. **Right**, quantification of Cav-1_{EC}:$TRPV4_{EC}$ co-localization in PAs of mice exposed to N (without and with SIN-1, PN donor, 50 µmol/L), CH or Su+CH conditions (n = 5). PAs from Cav-$1_{EC}^{-/-}$ mice were used as controls.

Supplemental Figure 12

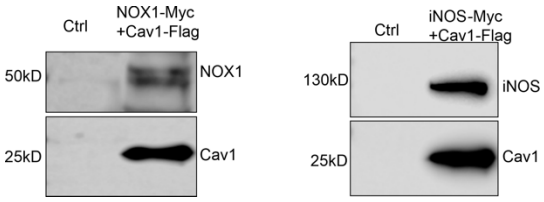

Supplemental Figure 12. Co-immunoprecipitation of iNOS or NOX1 with Cav-1 in HEK293T cells. HEK293T cells were co-transfected with plasmids expressing either NOX1-Myc and Cav1-Flag or iNOS-Myc and Cav1-flag for 48 hours. Cellular lysates were immunoprecipitated using anti-Myc magnetic beads and immunoblotted with Flag-HRP antibodies. Cell lysates from HEK293T cells that were not transfected with Cav1-Flag or iNOS-Myc or NOX1-Myc were used as negative control (Ctrl). Experiments were repeated 3 times.

Supplemental Figure 13

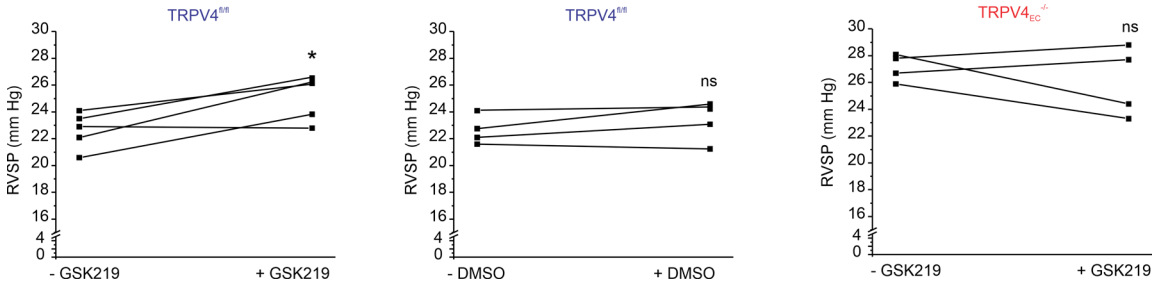

Supplemental Figure 13. Acute administration of TRPV4 inhibitor increases RVSP. *Left,* RVSP values before and 10 minutes after the administration of GSK219 (TRPV4 inhibitor, 10 mg/kg, i.p.) in TRPV4$^{fl/fl}$ mice (*P<0.05, n=5, paired t-test). *Middle,* RVSP values before and after the administration of DMSO (vehicle, n=4). *Right*, RVSP values before and after the administration of GSK219 in TRPV4$_{EC}^{-/-}$ mice (n=4).

Supplemental Figure 14

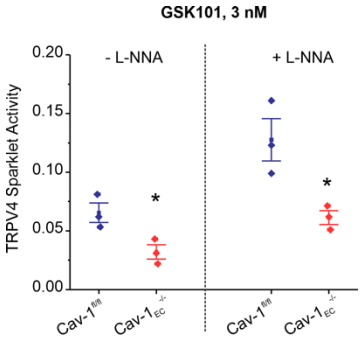

Supplemental Figure 14. The decreased activity of TRPV4$_{EC}$ channels is not due to altered NO levels in Cav-1$_{EC}^{-/-}$ mice. GSK101 (3 nmol/L)-induced TRPV4$_{EC}$ sparklet activity (NP_O) per site in *en face* preparations of PAs from Cav-1$^{fl/fl}$ or Cav-1$_{EC}^{-/-}$ mice in the absence or presence of L-NNA (NOS inhibitor; 100 μmol/L). Experiments were performed in the presence of cyclopiazonic acid (CPA; 20 μmol/L) to eliminate Ca^{2+} release from intracellular stores (n = 5; * *P* <0.05 vs. N [- L-NNA]; * *P* < 0.05 vs. N [- L-NNA]; t-test).

Reference List

1. Ottolini M*, et al.* (2020) Local Peroxynitrite Impairs Endothelial TRPV4 Channels and Elevates Blood Pressure in Obesity. *Circulation*.
2. Vandsburger MH*, et al.* (2007) Multi-parameter in vivo cardiac magnetic resonance imaging demonstrates normal perfusion reserve despite severely attenuated beta-adrenergic functional response in neuronal nitric oxide synthase knockout mice. *Eur Heart J* 28(22):2792-2798.
3. Anvari F*, et al.* (2010) Tissue-derived proinflammatory effect of adenosine A2B receptor in lung ischemia-reperfusion injury. *J Thorac Cardiovasc Surg* 140(4):871-877.
4. Ottolini M*, et al.* (2020) Local Peroxynitrite Impairs Endothelial Transient Receptor Potential Vanilloid 4 Channels and Elevates Blood Pressure in Obesity. *Circulation* 141(16):1318-1333.
5. Ottolini M*, et al.* (2020) Mechanisms underlying selective coupling of endothelial Ca(2+) signals with eNOS vs. IK/SK channels in systemic and pulmonary arteries. *J Physiol*.
6. Sonkusare SK*, et al.* (2012) Elementary Ca2+ signals through endothelial TRPV4 channels regulate vascular function. *Science* 336(6081):597-601.
7. Sonkusare SK*, et al.* (2014) AKAP150-dependent cooperative TRPV4 channel gating is central to endothelium-dependent vasodilation and is disrupted in hypertension. *Sci Signal* 7(333):ra66.
8. Marziano C*, et al.* (2017) Nitric Oxide-Dependent Feedback Loop Regulates Transient Receptor Potential Vanilloid 4 (TRPV4) Channel Cooperativity and Endothelial Function in Small Pulmonary Arteries. *J Am Heart Assoc* 6(12).
9. Liu Y*, et al.* (2002) Peroxynitrite inhibits Ca2+-activated K+ channel activity in smooth muscle of human coronary arterioles. *Circ Res* 91(11):1070-1076.